Electronic Supplementary Material (ESI) for Journal of Materials Chemistry A

Supporting information for

Monodisperse Cu@PtCu Nanocrystals and Their Conversion to Hollow-PtCu Nanostructures for Methanol Electro-oxidation

Xiaoqing Huang,[†] Yu Chen,[†] Enbo Zhu,[†] Yuxi Xu[‡], Duan,[‡§] and Yu Huang*[†§]
Email: yhuang@seas.ucla.edu

Experimental Details

Chemicals: Platium (II) acetylacetonate ($Pt(acac)_2$, ≥99.99%), Copper(II) acetylacetonate ($Cu(acac)_2$, ≥99.99%), Iron(III) chloride hexahydrate ($FeCl_3 \cdot 6H_2O$, ≥99%), Ammonium chloride (NH_4Cl, 99.99%), Hexadecyltrimethylammonium chloride ($CH_3(CH_2)_{15}N(Cl)(CH_3)_3$, CTAC, >98.0%), Ascorbic acid ($C_6H_8O_6$, AA, reagent grade), Benzoic acid (C_6H_5COOH, ≥99.5%), tert-Butyl hydroperoxide solution (TBHP, 5.0-6.0 M in decane), and Oleylamine ($CH_3(CH_2)_7CH=CH(CH_2)_7CH_2NH_2$, 70%) were all purchased from Sigma-Aldrich. All the chemicals were used as received without further purification. The water (18 MΩ/cm) used in all experiments was prepared by passing through an ultra pure purification system (Aqua Solutions).

Synthesis of hexagonal Cu@PtCu nanocrystals: In a typical synthesis of Cu@PtCu nanocrystals, Platium (II) acetylacetonate ($Pt(acac)_2$, 10.0 mg), Copper (II) acetylacetonate ($Cu(acac)_2$, 13.3 mg), Iron(III) chloride hexahydrate ($FeCl_3 \cdot 6H_2O$, 13.5 mg), Ascorbic acid ($C_6H_8O_6$, 35.2 mg) and 5 mL Oleylamine were added into a vial. After the vial had been capped, the mixture was ultrasonicated for around 15 minutes. The resulting homogeneous mixture was then heated from room temperature to 170 ºC in 15 min and kept at 170 ºC for 3 hours in an oil bath before it was cooled to room temperature. The resulting colloidal products were collected by centrifugation and washed with a hexane/ethanol mixture.

Preparation of hollow-PtCu/C catalysts: Typically, Cu@PtCu nanocrystals (10 mg in 5 mL hexane) were mixed with Ketjen carbon (C, 10 mg) suspended in hexane (10 mL). The mixture was ultrasonicated for 1 h. Tert-Butyl hydroperoxide solution (0.1 mL) and benzoic acid (61 mg) were added into the mixture after the sonication. The mixture was stirred at room temperature overnight. Finally, the hollow-PtCu/C catalysts was separated by centrifugation, washed five times with hexane/ethanol mixture, and redispersed in ethanol for electro-catalytic tests.

Electrochemical Measurements:

A three-electrode cell was used to do the electrochemical measurements. The working electrode was a glassy-carbon Electrode (RDE) (diameter: 5 mm, area: 0.196 cm^2) from Pine Instruments. Ag/AgCl (3 M Cl^-) was used as reference electrode. Pt wire was used as counter electrode. 40 μL Ethanol dispersion of hollow-PtCu/C catalyst (0.1 mg_{Pt}/mL) was deposited on a glassy carbon electrode to obtain the working electrode after the solvent is dried naturally. 5 μL of Nafion solution (0.1%) was dropped on the surface of the above catalysts modified RDE and dried naturally before electrochemical experiments. Therefore, the Pt loading of hollow-PtCu/C catalyst was 20.4 μg/cm^2. The electrochemical activity of the hollow-PtCu/C catalyst was characterized by cyclic voltammetry (CV) and chronoamperometry (CA) techniques. The electrochemical active surface area (EASA) measurement was determined by integrating the hydrogen adsorption charge on the CV at room temperature in 0.5 M H_2SO_4 solution. The potential scan rate was 50 mV/s for the CV measurement. Methanol oxidation experiment was carried out in a solution containing 0.5 M H_2SO_4 and 1.0 M CH_3OH with a scan rate of 50 mV/s. CA curves were recorded at 0.60 V in a solution containing 0.5 M H_2SO_4 and 1.0 M CH_3OH for 1000 s to investigate the stability of the electrocatalysts. For comparison, commercial Pt/C catalyst (E-TEK, 20 wt% Pt) was used as the baseline catalyst, and the same procedure as described above was used to conduct the electrochemical measurement, except that the Pt loadings were 17.9 $\mu g_{Pt}/cm^2$ for Pt/C catalyst and 20.4 μg/cm^2 for Solid-PtCu/C catalyst.

Characterization: TEM images were carried out on a FEI CM120 transmission electron microscope operated at 120 kV. High resolution TEM images and the high-angle annular dark-field scanning transmission electron microscope (HAADF-STEM)-energy-dispersive X-ray spectroscopy (EDS) was were taken on a FEI TITAN transmission electron microscope operated at 300 kV. The samples were prepared by dropping hexane or ethanol dispersion of samples onto carbon-coated copper TEM grids (Ted Pella, Redding, CA) using pipettes and dried under ambient condition. Scanning electron microscopic (SEM) images were taken on a JEOL JSM-6700F with field emission gun. X-ray powder diffraction patterns were collected on a Panalytical X'Pert Pro X-ray Powder Diffractometer with Cu-Kα radiation. The mole ratio of nanostructures was determined by the inductively coupled plasma atomic emission spectroscopy (TJA RADIAL IRIS 1000 ICP-AES).

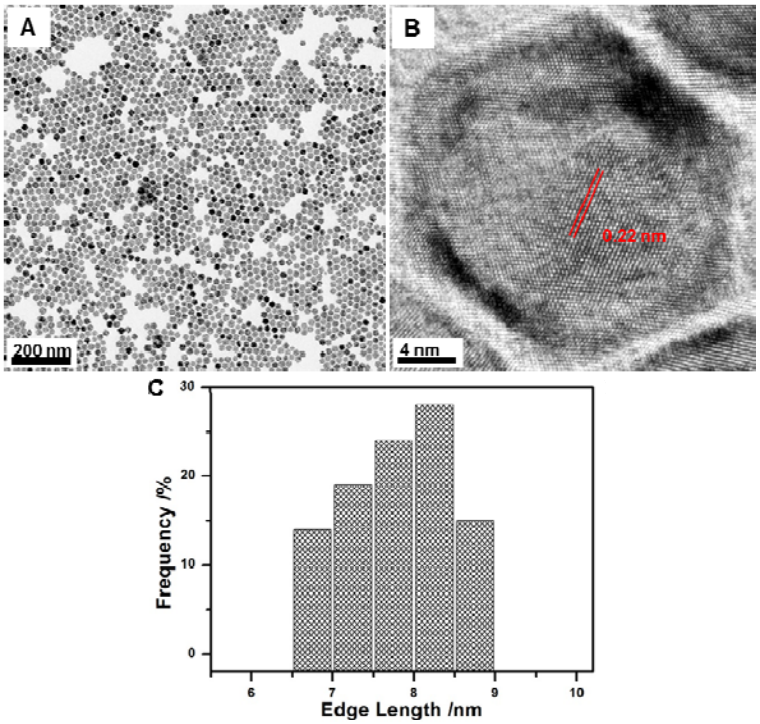

Figure S1. (A) Additional TEM image of Cu@PtCu nanocrystals, (B) HRTEM image of an individual Cu@PtCu nanocrystal and (C) the size distribution of Cu@PtCu nanocrystals.

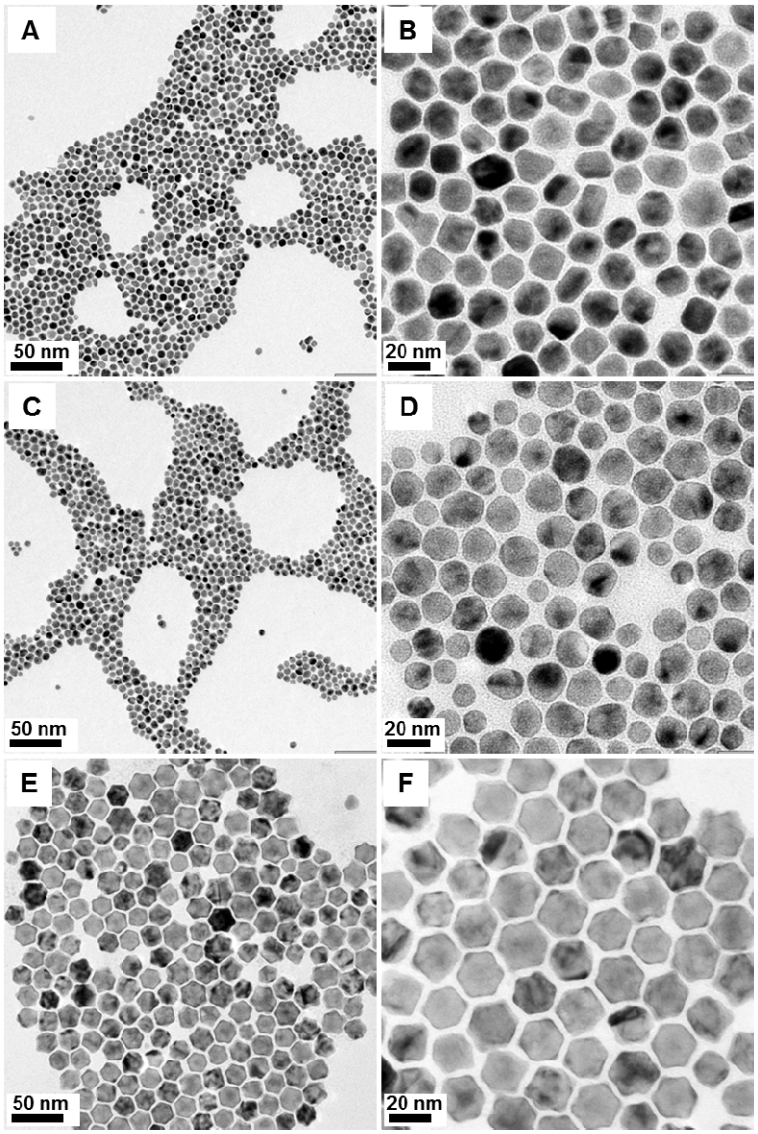

Figure S2. Representative TEM images of the products collected from the reaction with the same condition used in the synthesis of Cu@PtCu nanocrystals nanocrystals but (A, B) in the absence, (C, D) 2.7 mg and (E, F) 27.0 mg of $FeCl_3$.

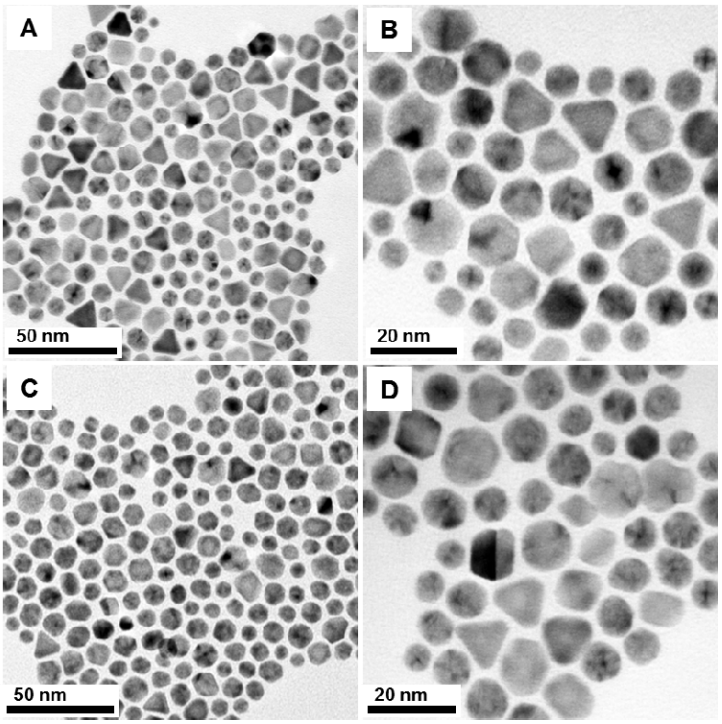

Figure S3. Representative TEM images of the products collected from the reaction with the same condition used in the synthesis of Cu@PtCu nanocrystals nanocrystals but changing $FeCl_3$ into (A, B) NH_4Cl and (C, D) CTAC.

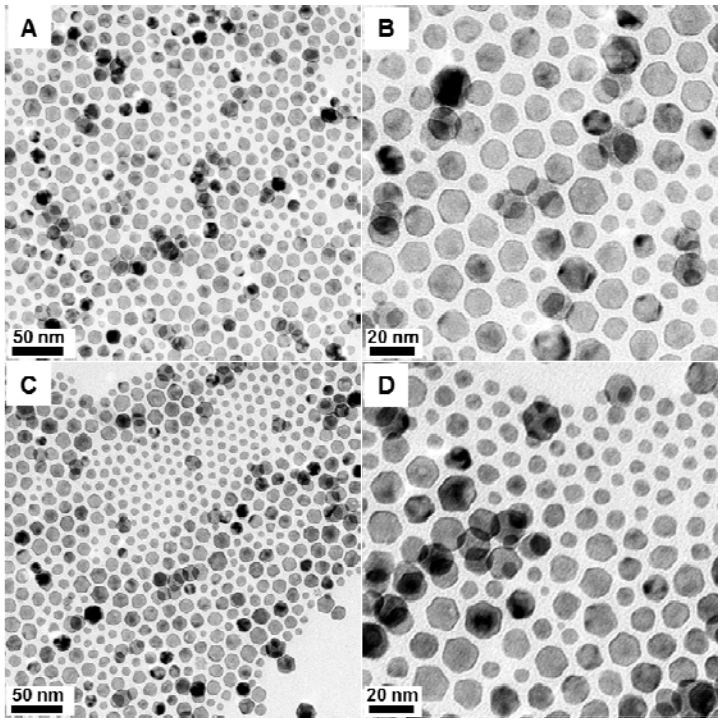

Figure S4. Representative TEM images of the products collected from the reaction with the same condition used in the synthesis of Cu@PtCu nanocrystals nanocrystals but (A, B) 6.7 mg and (C, D) 26.6 mg of $Cu(acac)_2$.

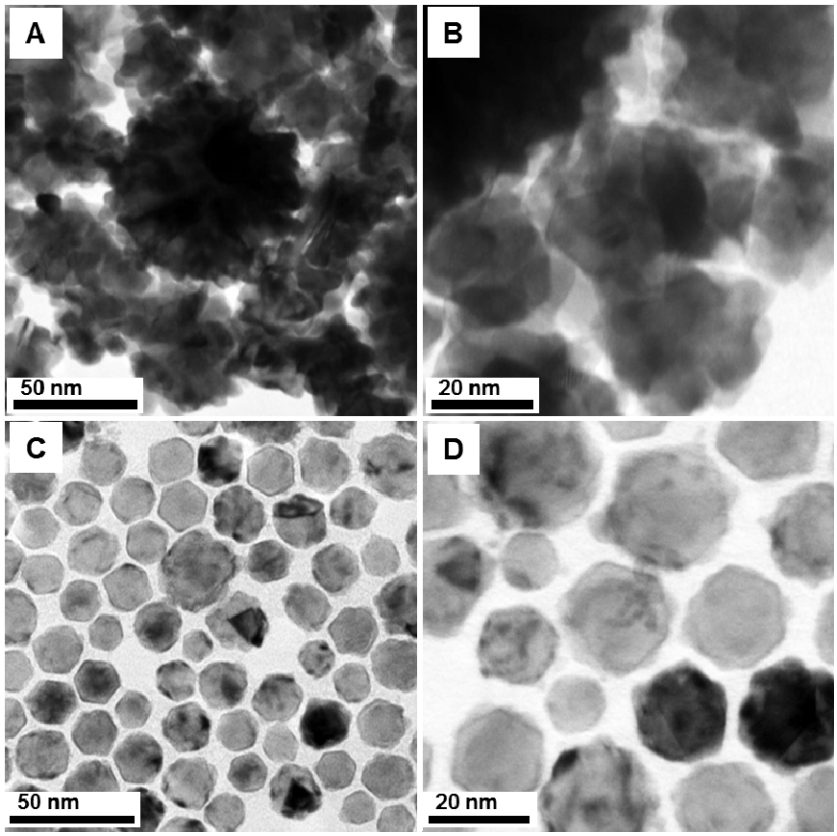

Figure S5. Representative TEM images of the products collected from the reaction with the same condition used in the synthesis of Cu@PtCu nanocrystals but (A, B) in the absence and (C, D) 8.8 mg of ascorbic acid (AA).

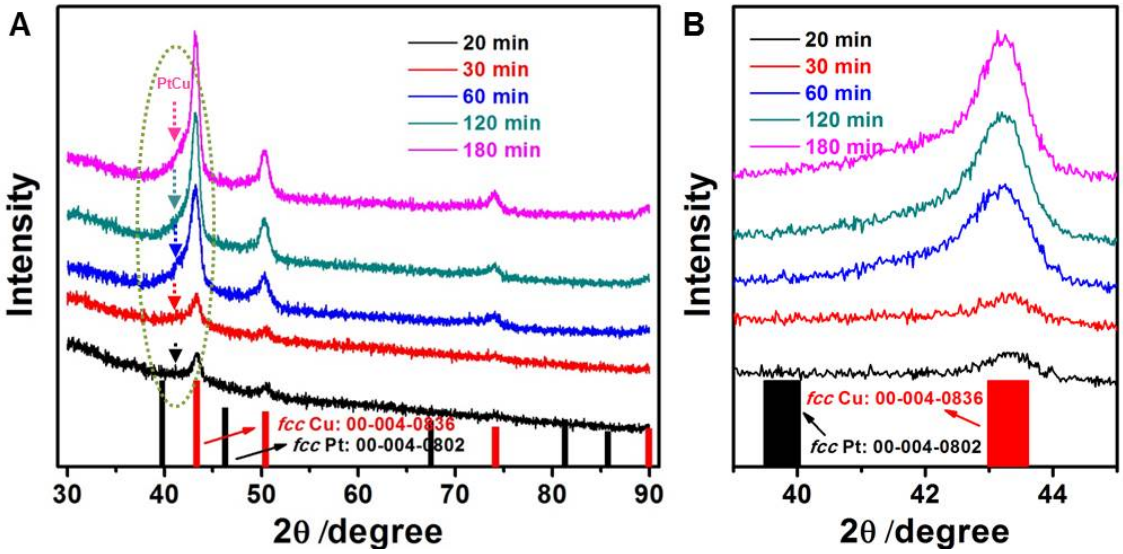

Figure S6. (A) XRD patterns (B) enlarged XRD patterns in the dashed circle of Figure S6A of the intermediate of Cu@PtCu nanocrystals collected from different reaction times.

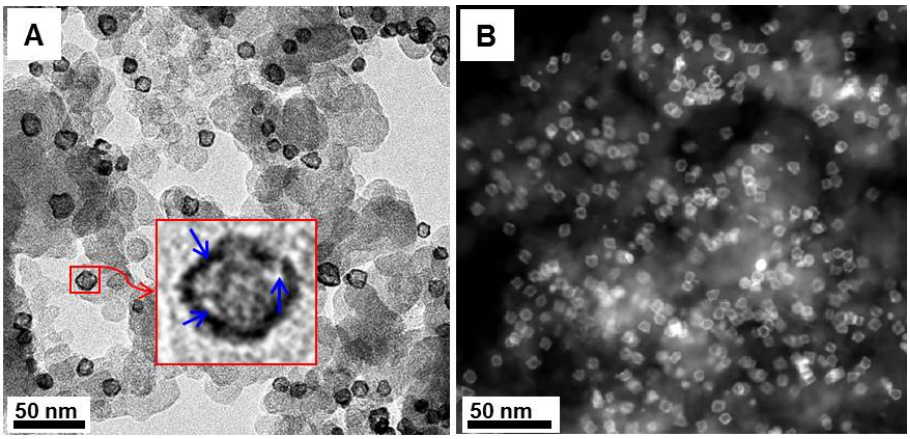

Figure S7. Additional TEM (A) and HAADF-STEM (B) images of hollow-PtCu/C nanocrystals. As shown in Figure S7A inset, micropore structure can be observed clearly.

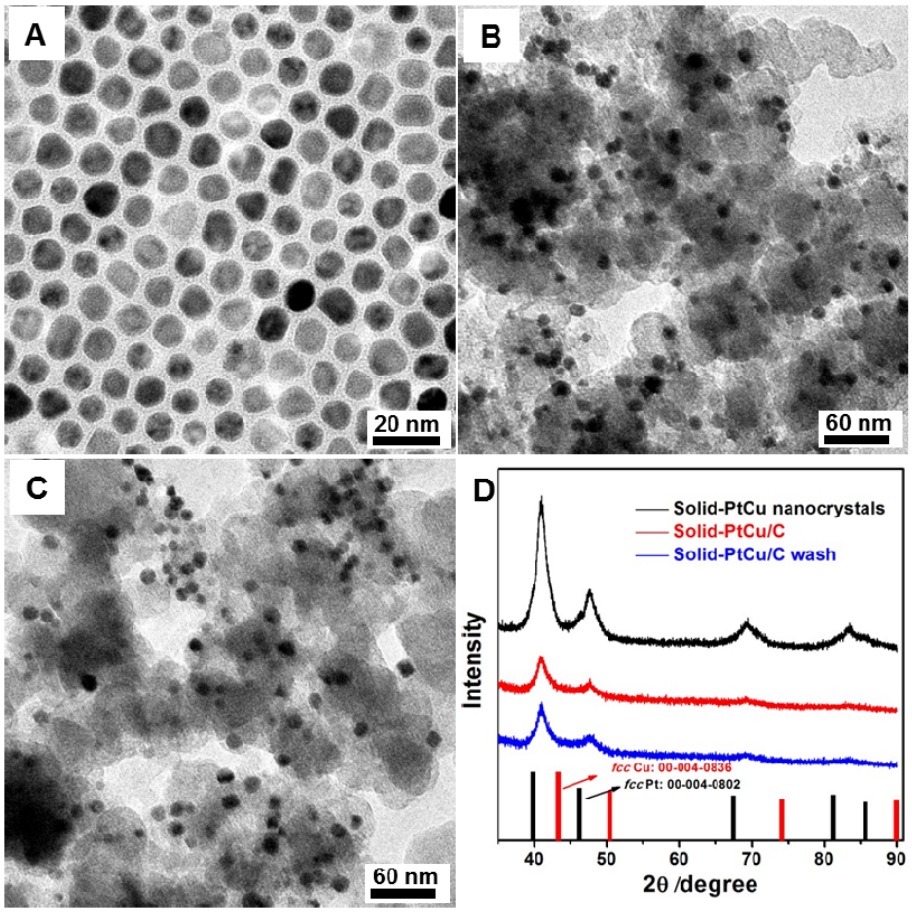

Figure S8. TEM images of (A) solid-PtCu nanocrystals, (B) solid-PtCu/C and (C) solid-PtCu/C after wash. (D) PXRD patterns of solid-PtCu, solid-PtCu/C and solid-PtCu/C after wash. The products were prepared from the reaction with the same condition used in the synthesis of Cu@PtCu nanocrystals nanocrystals but in the absence of $FeCl_3$ and the amount of $Cu(acac)_2$ is 6.7 mg.

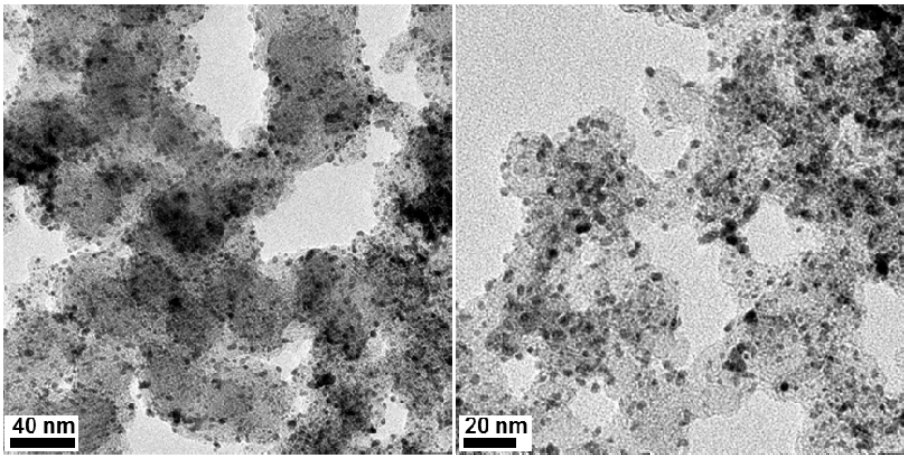

Figure S9. Representative TEM images of the commercial Pt/C.

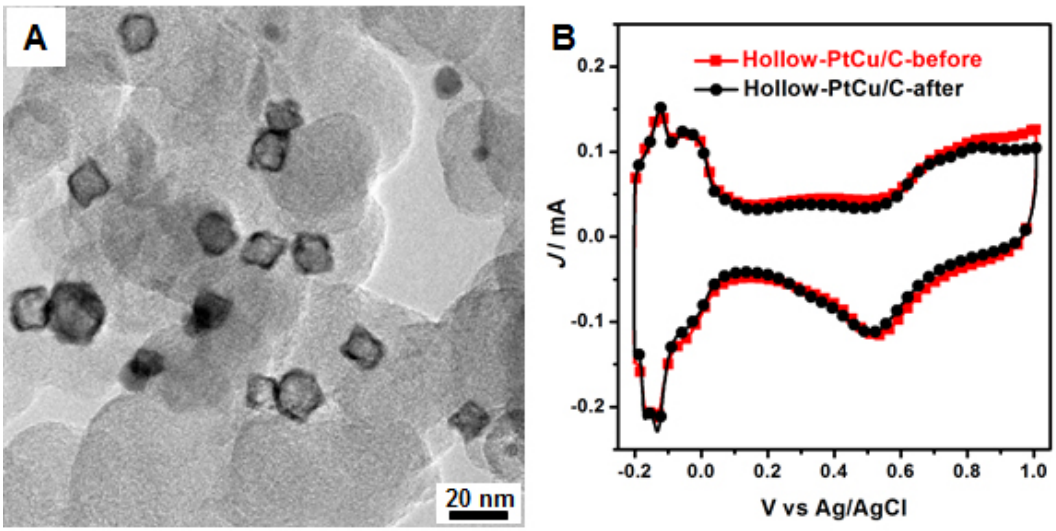

Figure S10. (A) Representative TEM image of the hollow-PtCu/C after 1000 s CA measurement and (B) CV curves of the hollow-PtCu nanocrystals before and after durability test.